NASA TECHNICAL NOTE

NASA TN D-3075

NASA TN D-3075

FATIGUE OF RENÉ 41 UNDER CONSTANT- AND RANDOM-AMPLITUDE LOADING AT ROOM AND ELEVATED TEMPERATURES

by Edward P. Phillips

Langley Research Center
Langley Station, Hampton, Va.

NATIONAL AERONAUTICS AND SPACE ADMINISTRATION • WASHINGTON, D. C. • NOVEMBER 1965

NASA TN D-3075

FATIGUE OF RENÉ 41 UNDER CONSTANT- AND RANDOM-AMPLITUDE LOADING AT ROOM AND ELEVATED TEMPERATURES

By Edward P. Phillips

Langley Research Center
Langley Station, Hampton, Va.

NATIONAL AERONAUTICS AND SPACE ADMINISTRATION

For sale by the Clearinghouse for Federal Scientific and Technical Information
Springfield, Virginia 22151 – Price $2.00

FATIGUE OF RENÉ 41 UNDER CONSTANT- AND RANDOM-AMPLITUDE LOADING AT ROOM AND ELEVATED TEMPERATURES

By Edward P. Phillips
Langley Research Center

SUMMARY

Narrow-band random-amplitude and constant-amplitude bending fatigue tests were conducted on sharply notched René 41 specimens at room temperature, 700° F (644° K), and 1400° F (1033° K). When compared on the basis of the root mean square of the nominal peak stresses, the random loading generally gave shorter lives than the constant-amplitude loading. Theoretical life predictions were made for the random-loading tests by using the Palmgren-Miner cumulative-damage rule and two different peak stress distributions (the distribution determined from the tests and the classical Rayleigh distribution). The predictions underestimated the fatigue life in practically all cases. The predicted lives based on the Rayleigh peak distribution were always less than those predicted by using the experimentally determined peak distribution. For both types of loading in the long-life region, a loss of fatigue strength from that at room temperature occurred at 700° F (644° K) but no further loss occurred at 1400° F (1033° K).

INTRODUCTION

The prediction of the fatigue life of structures subjected to random loadings represents a challenging problem to present-day designers of aircraft and missiles. A particular vehicle may receive random loadings from several sources, each loading being characterized by a power spectrum of different magnitude and shape. At the present time no analytical methods are available to give accurate and consistent answers in this problem area even for materials for which the constant-amplitude fatigue properties are well-known. To make the problem even more difficult, the high-temperature environments in which many new vehicles must operate necessitate the use of new materials for which few fatigue data of any kind are available. A remedy to this situation is, of course, to conduct test programs employing representative random loadings and temperatures.

One material which is being considered for high-temperature structural applications is René 41, a nickel-base superalloy. Some constant-amplitude axial-load fatigue data are available and have been published in reference 1. The purpose of the present investigation was to compare the fatigue properties of René 41 under constant- and random-amplitude loading at room temperature (≈78° F or ≈299° K), 700° F (644° K), and 1400° F (1033° K). All tests were

conducted on sharply notched cantilever-beam specimens with the loading applied at the free end. The stress response in the random-loading tests was narrow band in frequency and is representative of a structure for which a natural frequency occurs within the frequency range of the random-loading spectrum. Theoretical life predictions were made for the random-loading tests by using the Palmgren-Miner cumulative-damage theory. Two peak stress distributions were used in making the predictions, the distribution determined from the tests and, for comparison, the classical Rayleigh distribution which is often assumed for narrow-band stress response. (See refs. 2, 3, and 4.)

SYMBOLS

The units used for the physical quantities defined in this paper are given both in the U.S. Customary units and in the International System of Units (SI). (See ref. 5.) The Appendix presents factors relating these two systems of units.

n	number of cycles applied at a given nominal peak stress
N	experimental life of fatigue specimen under constant-amplitude loading, cycles
N_F	theoretical life of fatigue specimen under random-amplitude loading, cycles
P_b	probability of stress peaks occurring in stress band
$\left(\overline{S^2}\right)^{1/2}$	root-mean-square nominal stress, ksi (MN/m^2)
S_p	nominal peak stress, ksi (MN/m^2)
$\left(\overline{S_p^2}\right)^{1/2}$	root mean square of nominal peak stresses, ksi (MN/m^2)
ρ	notch root radius, inches (cm)

TESTS

Specimens

The specimen configuration used in this investigation is shown in figure 1. The dimensions shown in the figure are nominal; the actual dimensions used for computing section properties were determined by measuring to the nearest 0.0001 inch (3 μm). This edge-notched configuration corresponds to a theoretical elastic-stress concentration factor of approximately 7 for an axially loaded specimen.

The René 41 material was obtained as nominal 3/16-inch (0.48-cm) thick sheet in the mill-annealed condition. The specimen blanks were sheared from the sheet with the longitudinal axis of the specimen parallel to the direction of rolling. The blanks were heat treated before machining according to the following procedures:

(1) Heat to 1950° F (1339° K); maintain temperature for 30 minutes

(2) Air cool to room temperature

(3) Heat to 1400° F (1033° K); maintain temperature for 16 hours

(4) Air cool to room temperature

This heat treatment was used to obtain maximum tensile strength. After heat treatment, the specimens were machined from the blanks, material being taken from all surfaces to remove the oxide film resulting from heat treatment. The finished specimens had a surface finish of approximately 0.0001 inch (3 μm) root mean square.

The tensile properties and nominal chemical composition of René 41 are given in tables I and II, respectively. The tensile properties were obtained from the present investigation and from reference 6.

Test Equipment and Procedure

All tests were conducted by using electromagnetic shakers as a means of loading. A 25-lbf (111-N) vector-force shaker was used for the random-loading tests and an 8-lbf (36-N) vector-force shaker for the constant-amplitude tests. The free end of the cantilevered specimen was attached to the shaker drive coil by means of a rod and flexible connector. The flexible connector minimized longitudinal and torsional loading of the specimen. A room-temperature test setup is shown in figure 2. A schematic of the testing machines is shown in figure 3.

Method of stress calibration.- The moving core of a linear variable differential transformer (LVDT) was rigidly attached to the drive coil of the shaker. Any displacement of the drive coil caused a change in the output of the LVDT. For each test, a specimen was alined in the grips and secured to the drive coil of the shaker. The load required to produce a desired nominal test-section stress was computed with the flexure formula and was applied statically by dead-weight loading. The change in output of the LVDT was recorded and used as the set point in the ensuing test. The stresses presented in this report are nominal stresses as calculated from the measured displacements by means of the flexure formula and thus do not take into account the effects of plasticity.

Random loading.- The input signals to the shaker for the random-loading tests were repetitions of a magnetic-tape recording of a 6.4-second sample of the noise produced by a 2-inch (5.1-cm) subsonic cold-air jet. The recording was frequency modulated so that wear of the tape would not affect the magnitude of the signal. This signal had been used previously in the fatigue

investigation in references 7 and 8. No significance is attached to using this particular signal in this investigation except that it is random and rather wide band in frequency.

Fifty-eight specimens were tested at zero mean stress, various root-mean-square stress (LVDT output) levels, and the three temperature levels. The root-mean-square stress was held constant at the calibration set point throughout each test. An automatic cutoff was provided to shut down the equipment when the specimen failed. Time to failure was recorded for each test.

Tests were monitored by using a root-mean-square (rms) voltmeter and an oscilloscope. An estimated maximum error of 5 percent on root-mean-square nominal stress was possible in the tests since the indicating needle of the root-mean-square voltmeter was continuously in motion and this motion had to be centered about the desired value by the person conducting the test.

Samples of the shaker input and stress-response signals were recorded simultaneously at the start of each test.

Constant-amplitude loading.- The input to the shaker for these tests was a sinusoidal signal from an oscillator which was adjusted to operate near the natural frequency of the specimen-shaker system. Sixty-seven specimens were tested at zero mean stress, various root-mean-square stress levels, and the three temperature conditions. The same techniques and equipment used in the random-loading tests were employed in conducting these tests.

Elevated-temperature testing.- For all tests the temperature was monitored and controlled with thermocouples which were spotwelded to the top of the fixed half of the grips. A calibration specimen with 9 thermocouples emplaced at the test section was used to determine the set point for the control thermocouple and to determine the length of time required to attain steady-state conditions.

Testing at 700° F (644° K) was accomplished by using commercially available tubular furnaces with a hole cut into the side to allow attachment of the forcing rod to the specimen. Power was supplied to the furnace through a powerstat which was regulated by a temperature controller-recorder unit. A test setup is shown in figure 4.

For testing at 1400° F (1033° K), the tubular furnaces proved to be too slow in heating; therefore, an apparatus employing quartz-tube radiant heaters and reflectors was built at the Langley Research Center. The temperature-control equipment was the same as that for the 700° F tests. A test setup is shown in figure 5.

RESULTS AND DISCUSSION

Stress Response for Random Loading

Typical power spectra of the shaker input (load) and the LVDT output (stress) are plotted in figures 6(a) and 6(b) with logarithmic vertical scales.

Samples of the time histories of these signals are also shown in figure 6(c). Although the shaker input was rather wide band in frequency, the specimen responded only to frequency components near its natural frequency. This type of response resulted in a stress history which was of essentially constant frequency but variable in amplitude.

Knowledge of the distribution of the peak stresses is important in characterizing the fatigue environment since the fatigue damage of a cycle of stress is generally considered to depend on stress amplitude rather than on the shape of the stress cycle. Therefore, distributions of peaks were obtained for several tests having different stress levels and temperatures. The distributions were obtained by recording the stress histories with a light-beam oscillograph and then manually measuring the distance of each peak from the mean over a 6.4-second sample. The root mean square of the peak stresses $\left(\overline{S_p^2}\right)^{1/2}$ was calculated from the measurements. For the first test, both positive and negative peaks were measured. The analysis, however, showed that the positive and negative peak distributions were practically the same; thus, for subsequent tests, only the positive peak distribution was obtained. The results of the measurements are shown in figure 7 in terms of $S_p \Big/ \left(\overline{S_p^2}\right)^{1/2}$ and in percent of peaks exceeding S_p. No trend due to stress level or temperature was noted from the distributions. An average distribution for all the tests is described by the dashed line drawn through the data. The solid line in the figure describes the Rayleigh distribution.

Test Results

The results of the random-loading tests are presented in table III and are plotted in figure 8 in terms of cycles to failure and root-mean-square nominal stress, the quantity measured in the test. The cycles to failure were not measured in the tests but were computed as the product of time to failure and the natural frequency of the specimen. Curves were faired through the data for each temperature condition.

The results of the constant-amplitude tests are presented in table IV and are plotted in figure 9 in terms of peak nominal stress and cycles to failure. The cycles to failure were computed by the same procedures as those for the random-loading tests. Curves were faired through the data for each temperature condition and extrapolated to higher stress levels since information was required at these levels for the theoretical predictions of random-loading results.

Theoretical Life Predictions

Theoretical life predictions were made for the random-loading tests based on the Palmgren-Miner linear cumulative-damage theory. To make the calculations, it was assumed that each positive peak stress was followed by a negative peak stress of the same magnitude. This assumption was justified since the

positive and negative peak distributions were practically identical and since the stress time history had the appearance of a modulated sine wave. The calculations were made for various values of the root mean square of the peak stresses.

Two life predictions were generated for each temperature condition; one using the measured peak distribution and, for comparison, one using the Rayleigh distribution. The method of calculation of predicted life for each distribution is as follows:

To calculate the theoretical cycles to failure by using the measured peak stress distribution, figure 7 was divided into small, equal bands of $\frac{S_p}{\left(\overline{S_p^2}\right)^{1/2}}$ and the probability P_b of peaks occurring in each band was determined. The probability of peaks occurring in each band was divided by the constant-amplitude life N at the band midpoint stress, and the resulting quotients were summed. The reciprocal of this sum gives the predicted life, or expressed mathematically is:

$$N_F = \left(\sum \frac{P_b}{N}\right)^{-1}$$

To calculate the cycles to failure by using the Rayleigh distribution, the same procedure was used except that the probability of peaks in each stress band was calculated by using the Rayleigh probability density function. The upper cutoff level in stress magnitudes included in these calculations was taken as the level at which $\frac{P_b}{N}$ did not change the sum of quotients by more than 0.1 percent. This method of calculation of theoretical fatigue life is essentially the same as that explained in reference 2.

Comparison of Results

Comparison of constant and random loading.- In order to compare the constant- and random-amplitude tests on the basis of peak stresses, the ordinates of figures 8 and 9 were converted to the root mean square of peak stresses and the faired curves were replotted in figures 10, 11, and 12. For the constant-amplitude tests, the root mean square of peak stresses is the same as the stress amplitude or S_p. In the case of the random-loading tests, the root-mean-square stress was converted to the root mean square of peak stresses by the relation

$$\left(\overline{S_p^2}\right)^{1/2} = \left(\overline{2S^2}\right)^{1/2}$$

This relation was developed in reference 7 and is based on the theory of reference 9 for the narrow-band response of a lightly damped single-degree-of-freedom system.

When compared at equal values of the root mean square of peak stresses, the mean lives under random loading were generally shorter than those under constant-amplitude loading, the difference increasing from high to low stress levels. The only case where life under random loading was longer than that under constant-amplitude loading was at 1400° F (1033° K) at the highest random-loading stress levels. (See fig. 12.)

Comparison of experimental and predicted lives.- The fatigue-life predictions for the random-loading tests were made by using the Palmgren-Miner concept of fatigue damage in which $\sum \frac{n}{N} = 1$ means total damage or fatigue failure. Two life predictions were made for each temperature condition; one used the measured peak stress distribution, and the other used the Rayleigh peak stress distribution. The results of the life predictions for room temperature, 700° F (644° K), and 1400° F (1033° K) are plotted in figures 10, 11, and 12, respectively. The life predictions made by using the measured peak distribution were always greater than those made by using the Rayleigh peak distribution; however, the difference between the life predictions was generally small.

In practically all cases, experimental lives were greater than those predicted by using either the measured peak distribution or the Rayleigh peak distribution. Since the predicted lives represent $\sum \frac{n}{N} = 1$, this result means that for practically all the random-loading tests, $\sum \frac{n}{N} > 1$.

A clear trend for $\sum \frac{n}{N}$ for narrow-band random loading with a zero mean has not emerged from the literature. This point is illustrated in the following table:

Source	Specimen material	Type of loading	Type of specimen	Trend for $\sum \frac{n}{N}$
Reference 3	2024 aluminum alloy	Bending	Central hole	<1
Reference 8	SAE 4130 normalized steel	Bending	Edge notched	<1
Reference 10	24 ST aluminum alloy	Bending	Circumferential notch	<1
Reference 11	2024 aluminum alloy	Bending	Circumferential notch	<1
Reference 12	2024-T3 aluminum alloy	Bending	Unnotched	<1
Reference 4	L.73 aluminum alloy	Axial	Unnotched	>1
Reference 7	7075-T6 aluminum alloy	Bending	Edge notched	>1
Present investigation	René 41	Bending	Edge notched	>1

A complete explanation cannot be given for the differences reported, but there is evidence that some of the differences in results could be due to the materials tested. For example, it has been reported in references 13 and 14 that for variable-amplitude tests with zero mean, 7075-T6 aluminum alloy gave consistently higher values of $\sum \frac{n}{N}$ than 2024-T3 aluminum alloy did. Of the investigations listed in the previous table, one used 7075 aluminum alloy and reported $\sum \frac{n}{N} > 1$, whereas four employed 2024 aluminum alloy and reported $\sum \frac{n}{N} < 1$. Adding to this evidence is the fact that the test programs of references 7 and 8 were practically identical except for specimen material and yet the tests resulted in different trends for $\sum \frac{n}{N}$.

Temperature effects.- For short lives, a progressive loss of fatigue strength occurred with increase in temperature, the greatest loss occurring between 700° F (644° K) and 1400° F (1033° K). (See figs. 8 and 9.) For longer lives, however, the curves for 700° F and 1400° F begin to converge and in the case of constant-amplitude loading, fatigue strength at 1400° F is higher than that at 700° F. The constant-amplitude S-N curve for 1400° F is marked by a very sharp break at the knee; this result, however, is based on a rather small number of data points.

The result that the fatigue strength did not progressively decrease with increase in temperature in the long-life region is not unique to René 41. Similar behavior has been reported for SAE 4340 steel in reference 15 and for PH15-7Mo stainless steel (Condition TH 1050) in reference 16.

CONCLUDING REMARKS

Narrow-band random-amplitude and constant-amplitude bending fatigue tests were conducted on sharply notched René 41 specimens. Tests were conducted at room temperature, 700° F (644° K), and 1400° F (1033° K). Theoretical life predictions were made for the random-loading tests by using the Palmgren-Miner cumulative-damage rule and two different peak stress distributions, the distribution determined from the tests and the classical Rayleigh distribution. From the data presented, the following observations are made:

1. When compared on the basis of the root mean square of peak nominal stresses, the random loading generally gave shorter fatigue lives than the constant-amplitude loading.

2. In practically all cases, the experimental lives were greater than those predicted by using either the measured peak stress distribution or the Rayleigh peak stress distribution.

3. The life predictions made by using the measured peak stress distribution were always greater than those made by using the Rayleigh distribution.

4. For short lives, a progressive loss of fatigue strength occurred with increase in temperature. For long lives, fatigue strength decreased from room temperature to 700° F (644° K) but did not decrease further at 1400° F (1033° K).

Langley Research Center,
National Aeronautics and Space Administration,
Langley Station, Hampton, Va., August 12, 1965.

APPENDIX

CONVERSION OF U.S. CUSTOMARY UNITS TO SI UNITS

The International System of Units (SI) was adopted by the Eleventh General Conference on Weights and Measures, Paris, October 1960, in Resolution No. 12 (ref. 5). Conversion factors for the units used herein are given in the following table:

Physical quantity	U.S. Customary Unit	Conversion factor (*)	SI unit
Length	in.	0.0254	meters (m)
Temperature	$^{o}F + 459.67$	5/9	degrees Kelvin (^{o}K)
Force	lbf	4.448	newtons (N)
Stress	psi = $lbf/in.^2$	6.895×10^3	newtons per sq meter (N/m^2)

*Multiply value given in U.S. Customary Unit by conversion factor to obtain equivalent in SI unit.

Prefixes to indicate multiple of units are as follows:

Prefix	Multiple
kilo (k)	10^3
mega (M)	10^6
giga (G)	10^9
centi (c)	10^{-2}
micro (μ)	10^{-6}

REFERENCES

1. Greene, A.; et al.: Research Investigation To Determine Mechanical Properties of Nickel and Cobalt-Base Alloys for Inclusion in Military Handbook 5. ML-TDR-64-116, vol. I, U.S. Air Force, Oct. 1964.

2. McClymonds, J. C.; and Ganoung, J. K.: Combined Analytical and Experimental Approach for Designing and Evaluating Structural Systems for Vibration Environments. Eng. Paper No. 3091, Missile and Space Systems Div., Douglas Aircraft Co., Oct. 1964.

3. Smith, P. W., Jr.; and Malme, C. I.: Fatigue Tests of a Resonant Structure With Random Excitation. J. Acoustical Soc. Am., vol. 35, no. 1, Jan. 1963, pp. 43-46.

4. Lowcock, M. T.; and Williams, T. R. G.: Effect of Random Loading On the Fatigue Life of Aluminum Alloy L.73. A.A.S.U. Rept. No. 225, Univ. of Southampton (Hampshire, England), July 1962.

5. Mechtly, E. A.: The International System of Units - Physical Constants and Conversion Factors. NASA SP-7012, 1964.

6. Weiss, V.; and Sessler, J. G., eds.: Aerospace Structural Metals Handbook. Volume II - Non-Ferrous Alloys. ASD-TDR-63-741, Vol. II, U.S. Air Force, Mar. 1963. (Revised Mar. 1964.)

7. Fralich, Robert W.: Experimental Investigation of Effects of Random Loading on the Fatigue Life of Notched Cantilever-Beam Specimens of 7075-T6 Aluminum Alloy. NASA MEMO 4-12-59L, 1959.

8. Fralich, Robert W.: Experimental Investigation of Effects of Random Loading on the Fatigue Life of Notched Cantilever-Beam Specimens of SAE 4130 Normalized Steel. NASA TN D-663, 1961.

9. Miles, John W.: An Approach to the Buffeting of Aircraft Structures by Jets. Rept. No. SM-14795, Douglas Aircraft Co., Inc., June 1953.

10. Head, A. K.; and Hooke, F. H.: Random Noise Fatigue Testing. Proc. Int. Conf. on Fatigue of Metals (London and New York), Inst. Mech. Eng. and A.S.M.E., 1956, pp. 301-303.

11. Kowalewski, J.: On the Relation Between Fatigue Lives Under Random Loading and Under Corresponding Program Loading. Full-Scale Fatigue Testing of Aircraft Structures, F. J. Plantema and J. Schijve, eds., Pergamon Press, 1961, pp. 60-75.

12. Fuller, J. R.: Research on Techniques of Establishing Random Type Fatigue Curves for Broad Band Sonic Loading. ASD-TDR-62-501 (Contract AF 33(616)-8087), U.S. Air Force, Oct. 1962.

13. Naumann, Eugene C.; Hardrath, Herbert F.; and Guthrie, David E.: Axial-Load Fatigue Tests of 2024-T3 and 7075-T6 Aluminum-Alloy Sheet Specimens Under Constant- and Variable-Amplitude Loads. NASA TN D-212, 1959.

14. Naumann, Eugene C.: Variable-Amplitude Fatigue Tests With Particular Attention to the Effects of High and Low Loads. NASA TN D-1522, 1962.

15. Trapp, W. J.: Elevated Temperature Fatigue Properties of SAE 4340 Steel. WADC Tech. Rept. 52-325, Pt. 1, U.S. Air Force, Dec. 1952.

16. Illg, Walter; and Castle, Claude B.: Axial-Load Fatigue Properties of PH 15-7 Mo Stainless Steel in Condition TH 1050 at Ambient Temperature and 500° F. NASA TN D-2358, 1964.

TABLE I.- TENSILE PROPERTIES OF RENÉ 41 AT ROOM AND ELEVATED TEMPERATURES

Source	Temperature	Number of tests	Ultimate tensile strength		Yield strength (0.2% offset)		Elongation, percent	Modulus of elasticity	
			ksi	MN/m^2	ksi	MN/m^2		ksi	GN/m^2
Present investigation	Room	7	178 minimum	1228 minimum	128 minimum	883 minimum	11.0 minimum[a,b]	29.4×10^3 minimum	202.9 minimum
			182 average	1256 average	131 average	904 average	12.9 average[a,b]	30.4×10^3 average	210.0 average
			187 maximum	1290 maximum	135 maximum	932 maximum	15.5 maximum[a,b]	31.2×10^3 maximum	215.3 maximum
Reference 6	Room	---	185	1276	140	966	[c]18.2	30.2×10^3	208.4
	700° F (644° K)	---	180	1242	131	904	[c]16.5	27.3×10^3	188.4
	1400° F (1033° K)	---	149	1028	117	807	[c]14.8	20.2×10^3	139.4

[a]Based on 6 tests.
[b]2.00-inch (5.08-cm) gage length.
[c]No gage length given.

TABLE II.- NOMINAL CHEMICAL COMPOSITION OF RENÉ 41

Element	Percent
Carbon	0.06 to 0.12
Silicon	0.50 maximum
Manganese	0.50 maximum
Iron	5.00 maximum
Chromium	18.00 to 20.00
Boron	0.003 to 0.010
Cobalt	10.00 to 12.00
Molybdenum	9.00 to 10.50
Titanium	3.00 to 3.30
Aluminum	1.40 to 1.60
Nickel	Balance

end

TABLE III.- RESULTS OF RANDOM-LOADING FATIGUE TESTS OF RENÉ 41 SPECIMENS AT ROOM AND ELEVATED TEMPERATURES WITH ZERO MEAN STRESS

$(\overline{s^2})^{1/2}$		Time to failure	Natural frequency	Fatigue life
ksi	MN/m^2	Minutes	cps or Hz	Cycles
Room temperature				
52.8	364	8	106	50 880
50.0	345	10	107	64 200
50.0	345	12	108	77 760
50.0	345	14	101	84 840
40.0	276	32	101	193 920
40.0	276	36	101	218 160
40.0	276	46	105	289 800
30.0	207	112	110	739 200
30.0	207	120	104	748 800
30.0	207	125	102	765 000
30.0	207	114	112	766 080
30.0	207	152	103	939 360
30.0	207	192	103	1 186 560
25.0	172	281	105	1 770 300
25.0	172	310	104	1 934 400
25.0	172	507	106	3 224 520
20.0	138	431	103	2 663 580
20.0	138	860	105	5 418 000
20.0	138	1 010	109	6 605 400
20.0	138	2 397	106	15 244 920
20.0	138	3 612	106	22 972 320
20.0	138	12 902	108	83 604 960
17.0	117	4 671	107	29 987 820
15.0	104	>11 365	101	>68 871 900
700° F (644° K)				
37.5	259	30	104	187 200
36.7	253	21	102	128 200
30.0	207	96	98	564 480
30.0	207	94	103	580 920
30.0	207	81	100	486 000
30.0	207	80	102	489 600
28.3	195	52	108	336 960
20.0	138	443	102	2 711 160
20.0	138	578	103	3 572 040
20.0	138	729	98	4 286 520
20.0	138	811	103	5 011 980
17.0	117	894	107	5 739 480
15.0	104	1 749	102	10 703 880
15.0	104	2 724	102	16 670 880
15.0	104	3 840	103	23 731 200
13.0	90	3 984	102	24 382 080
13.0	90	5 076	98	29 846 880
10.0	69	>17 634	102	>107 920 080
1400° F (1033° K)				
26.3	181	35	98	205 800
25.0	172	43	97	250 260
25.0	172	55	96	316 800
20.0	138	96	98	564 480
20.0	138	107	95	609 900
20.0	138	130	94	733 200
15.0	104	276	99	1 639 440
15.0	104	463	94	2 611 320
15.0	104	466	96	2 684 160
15.0	104	539	100	3 234 000
13.0	90	671	95	3 824 700
13.0	90	702	97	4 085 640
13.0	90	825	96	4 752 000
13.0	90	1 833	97	10 668 060
11.0	76	11 556	94	65 175 840
10.0	69	>17 187	99	>102 090 780

TABLE IV.- RESULTS OF CONSTANT-AMPLITUDE FATIGUE TESTS OF RENÉ 41 SPECIMENS AT ROOM AND ELEVATED TEMPERATURES WITH ZERO MEAN STRESS

$\left(\overline{s^2}\right)^{1/2}$		Time to failure	Natural frequency	Fatigue life
ksi	MN/m^2	Minutes	cps or Hz	Cycles
Room temperature				
50.0	345	12	105	75 600
50.0	345	15	105	94 500
50.0	345	20	104	124 800
50.0	345	22	101	133 320
40.0	276	24	105	151 200
40.0	276	30	106	190 800
40.0	276	45	115	310 500
40.0	276	76	104	474 240
40.0	276	102	99	605 880
30.0	207	156	102	954 720
30.0	207	192	105	1 209 600
30.0	207	477	102	2 919 240
30.0	207	603	103	3 726 540
30.0	207	635	103	3 924 300
30.0	207	906	100	5 436 000
30.0	207	954	101	5 781 240
30.0	207	1 276	102	7 809 120
25.0	172	804	102	4 920 480
25.0	172	1 074	106	6 830 640
25.0	172	2 188	100	13 128 000
25.0	172	2 724	104	16 997 760
25.0	172	4 315	102	26 407 800
22.0	152	1 728	106	10 990 080
22.0	152	4 170	102	25 520 400
22.0	152	4 326	104	26 994 240
22.0	152	>17 346	103	>107 198 280
20.0	138	>18 098	104	>112 931 520
700° F (644° K)				
50.0	345	11	96	63 360
50.0	345	12	97	69 840
50.0	345	15	97	87 300
40.0	276	15	98	88 200
40.0	276	24	96	138 240
40.0	276	28	97	162 960
40.0	276	33	98	194 040
30.0	207	96	96	552 960
30.0	207	100	98	588 000
30.0	207	138	98	811 440
30.0	207	175	97	1 018 500
25.0	172	242	96	1 393 920
25.0	172	333	98	1 958 040
25.0	172	399	100	2 394 000
20.0	138	240	98	1 411 200
20.0	138	378	98	2 222 640
20.0	138	749	99	4 449 060
20.0	138	849	95	4 839 300
20.0	138	11 241	101	68 120 460
20.0	138	12 020	97	69 956 400
17.0	117	2 919	96	16 813 440
17.0	117	5 892	99	34 998 480
17.0	117	>18 601	98	>109 373 880
1400° F (1033° K)				
40.0	276	9	91	49 140
40.0	276	10	93	55 800
40.0	276	10	93	55 800
40.0	276	10	94	56 400
30.0	207	20	98	117 600
30.0	207	24	90	129 600
30.0	207	25	96	144 000
30.0	207	33	93	184 140
20.0	138	53	94	298 920
20.0	138	56	94	315 840
20.0	138	65	94	366 600
20.0	138	67	94	377 880
20.0	138	78	94	439 920
18.0	124	5 641	94	31 815 240
18.0	124	12 582	94	70 962 480
18.0	124	>17 802	93	>99 335 160
15.0	104	>18 213	94	>102 721 320

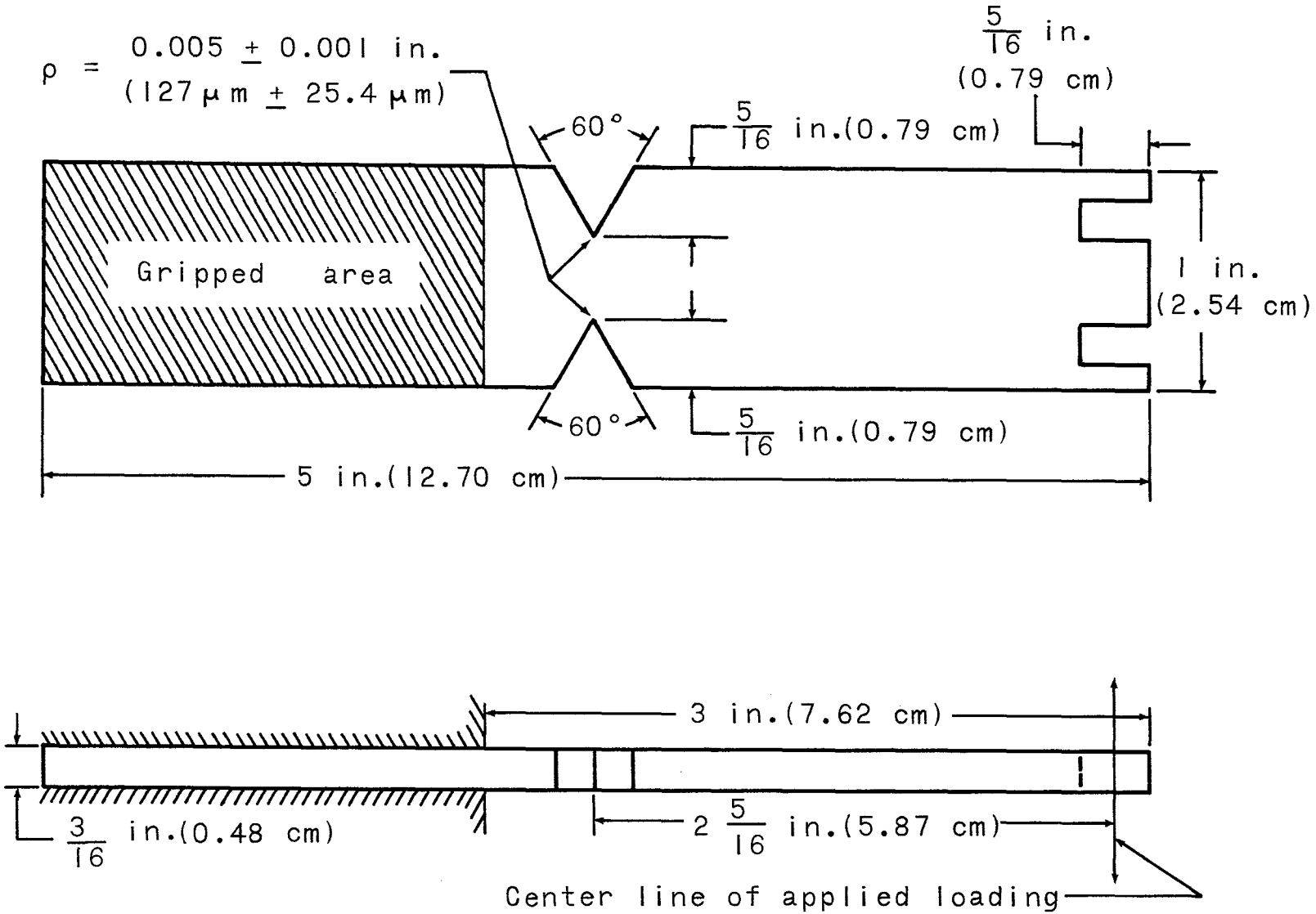

Figure 1.- Specimen configuration for fatigue tests on René 41.

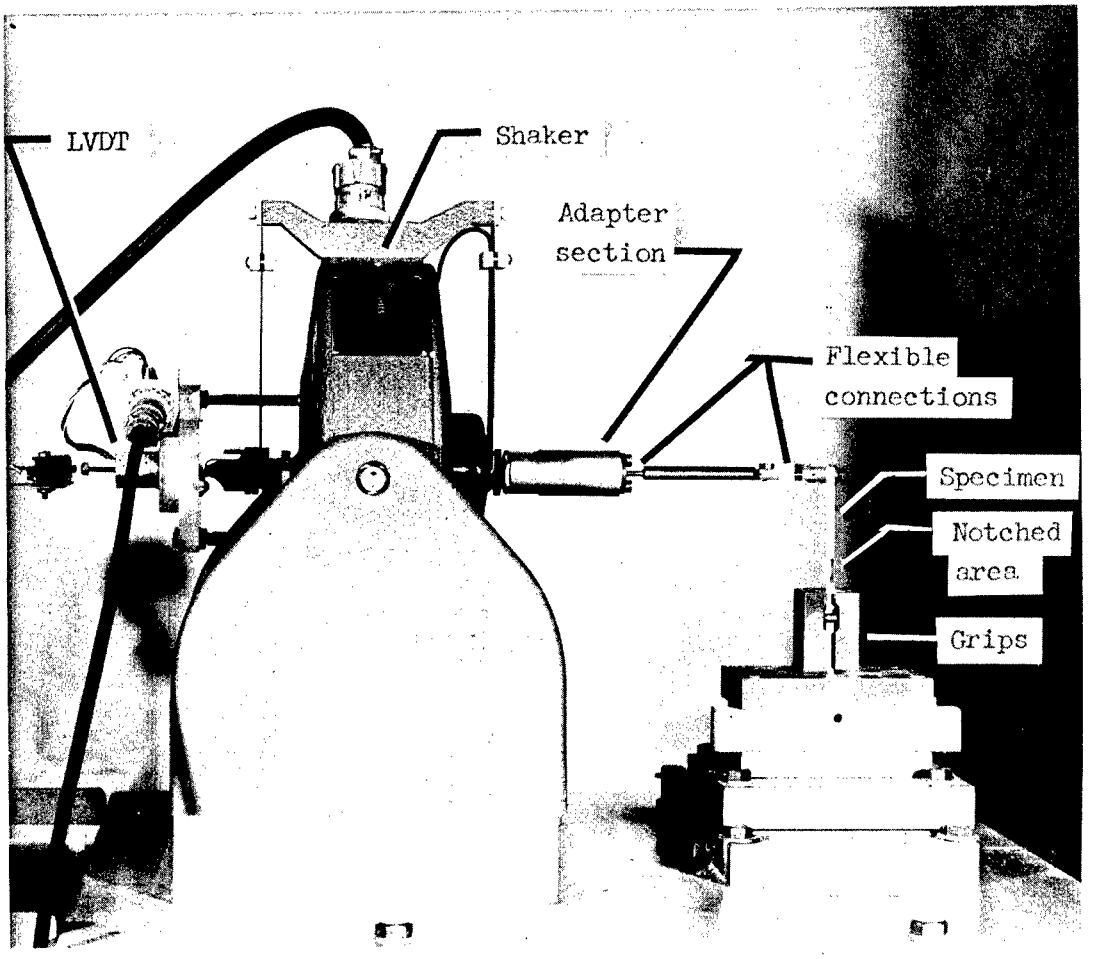

Figure 2.- Typical test setup for room-temperature fatigue test of René 41 specimen. L-64-1007.1

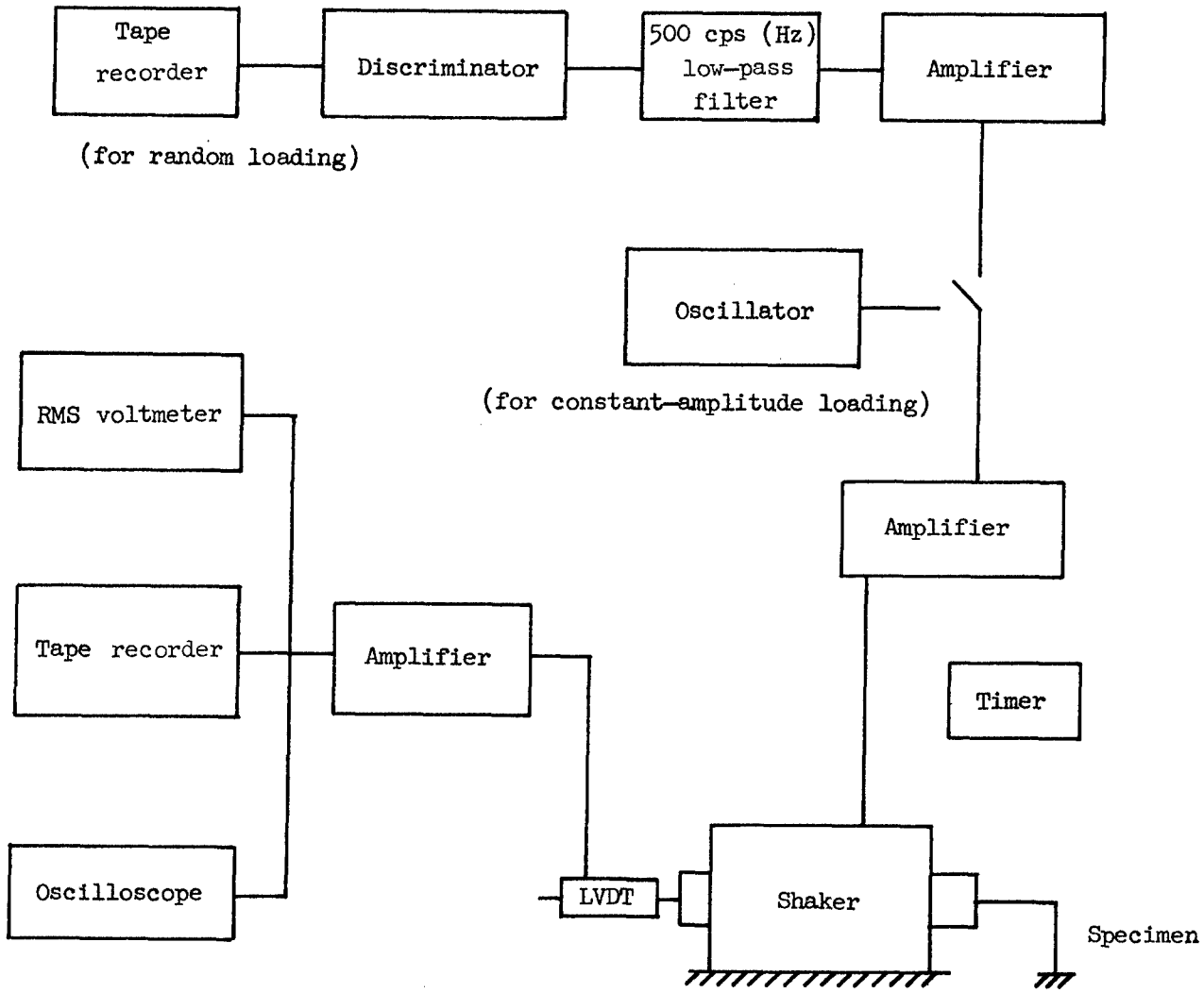

Figure 3.- Schematic of testing machines used in conducting fatigue tests.

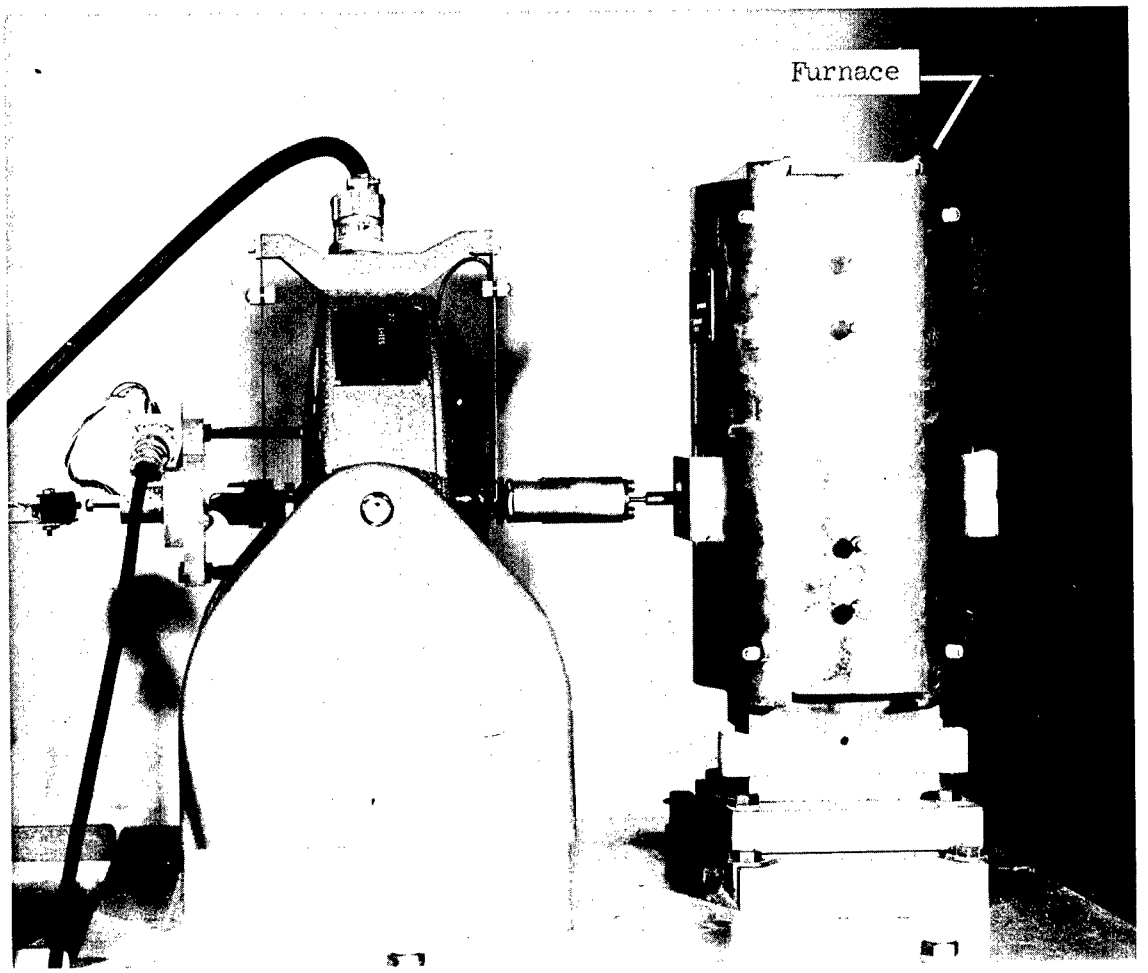

Figure 4.- Typical test setup for 700° F (644° K) fatigue test of René 41 specimen. L-64-1003.1

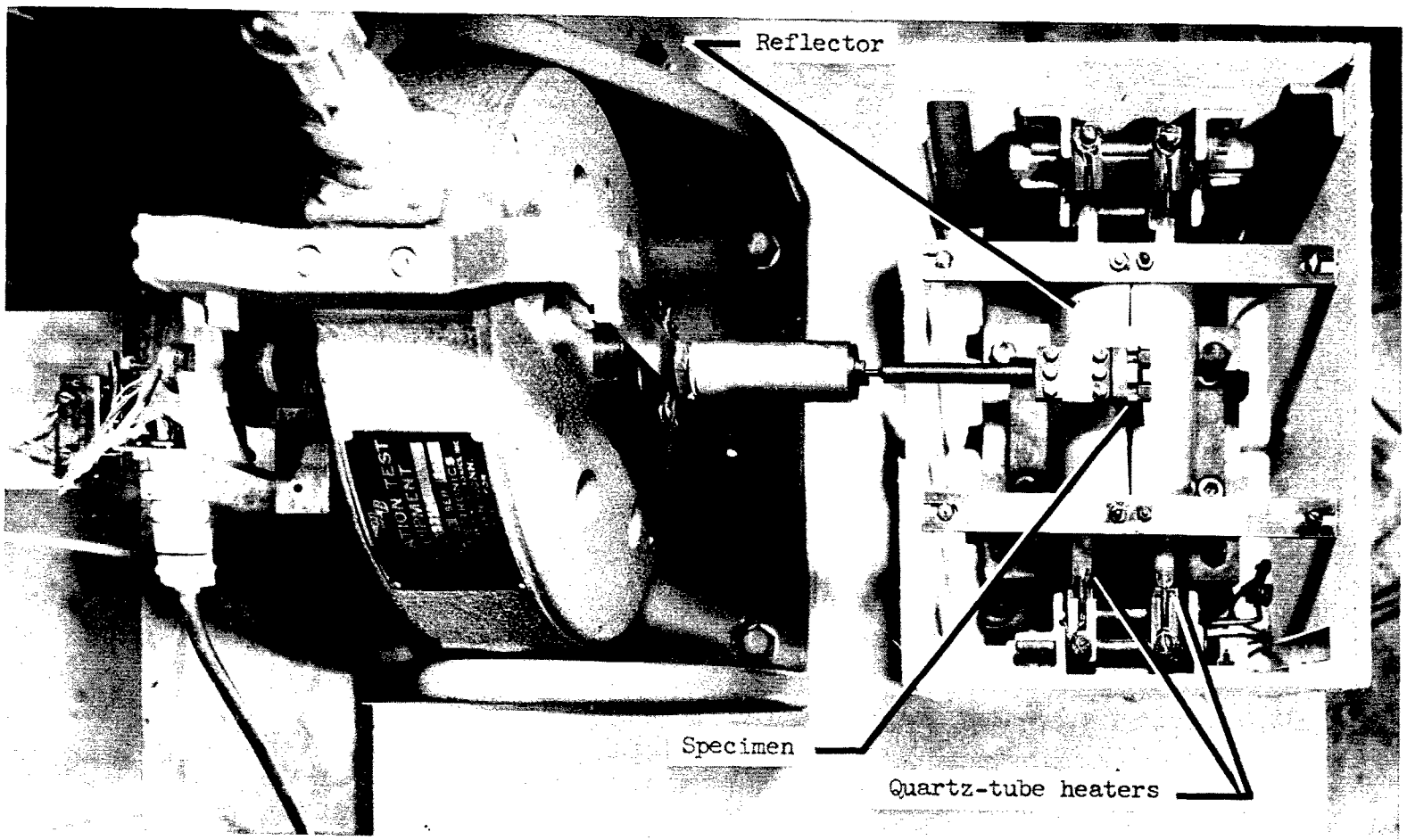

Figure 5.- Top view of typical test setup for 1400° F (1033° K) fatigue test of René 41 specimen.

L-64-1005.1

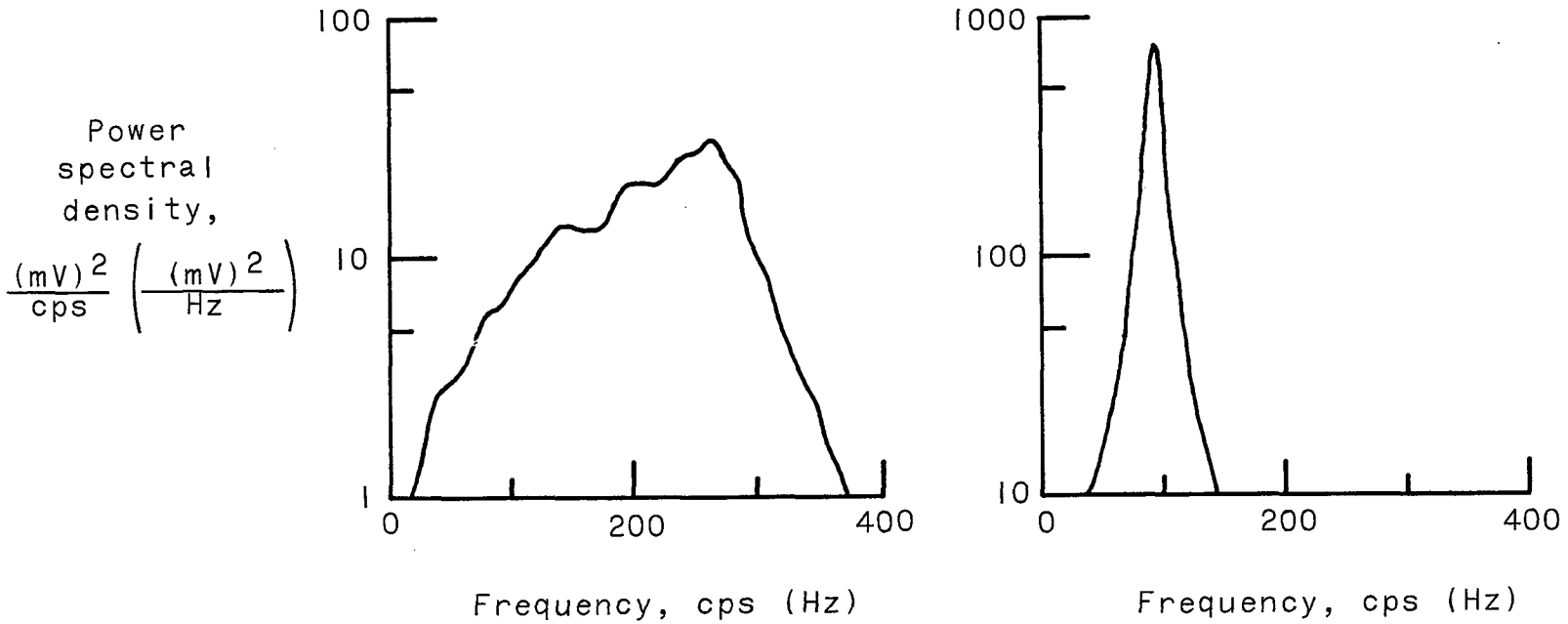

(a) Power spectrum of shaker input.

(b) Power spectrum of LVDT output.

Figure 6.- Characteristics of shaker input and LVDT output for typical random-loading test.

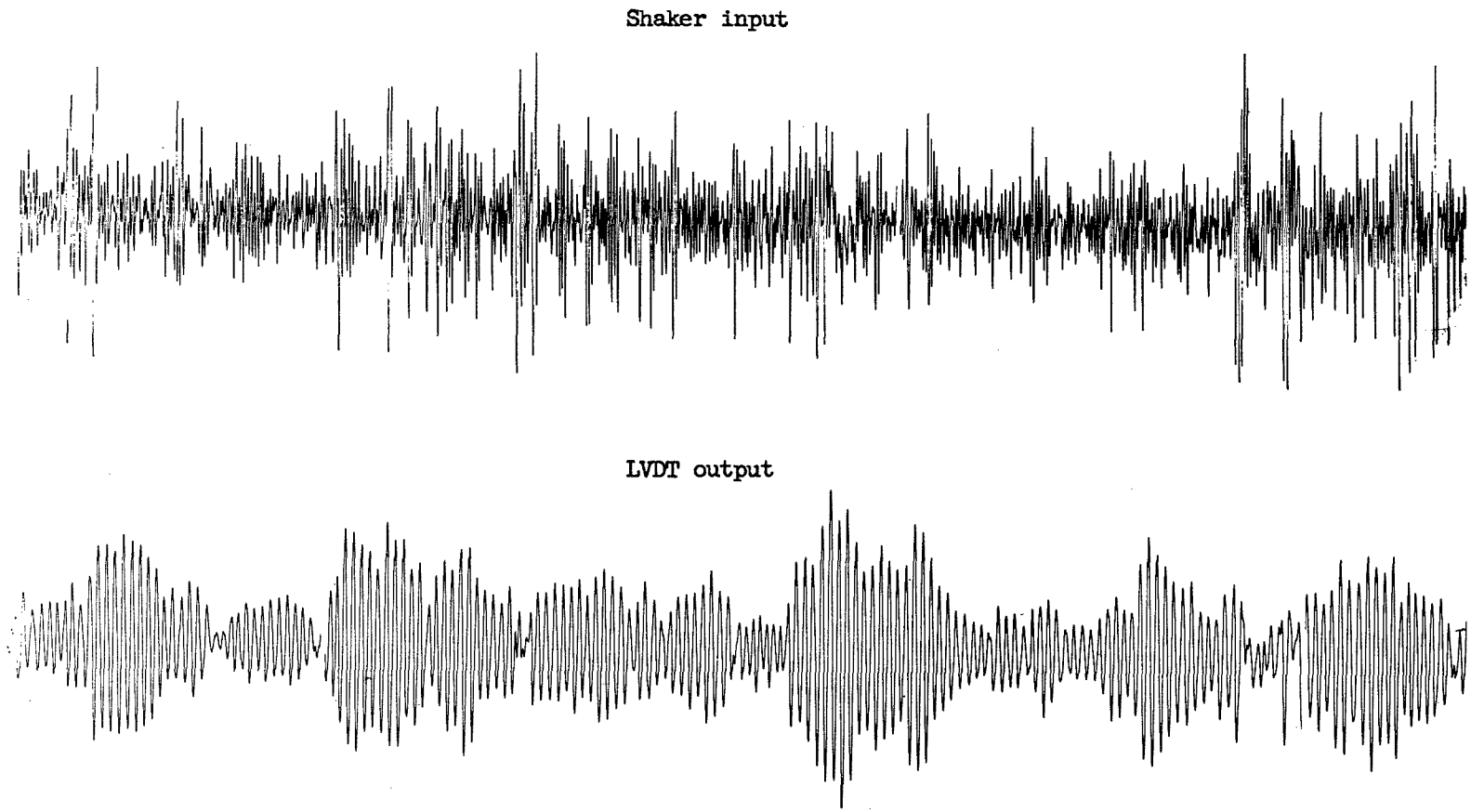

(c) Samples of time histories of shaker input and LVDT output.

Figure 6.- Concluded.

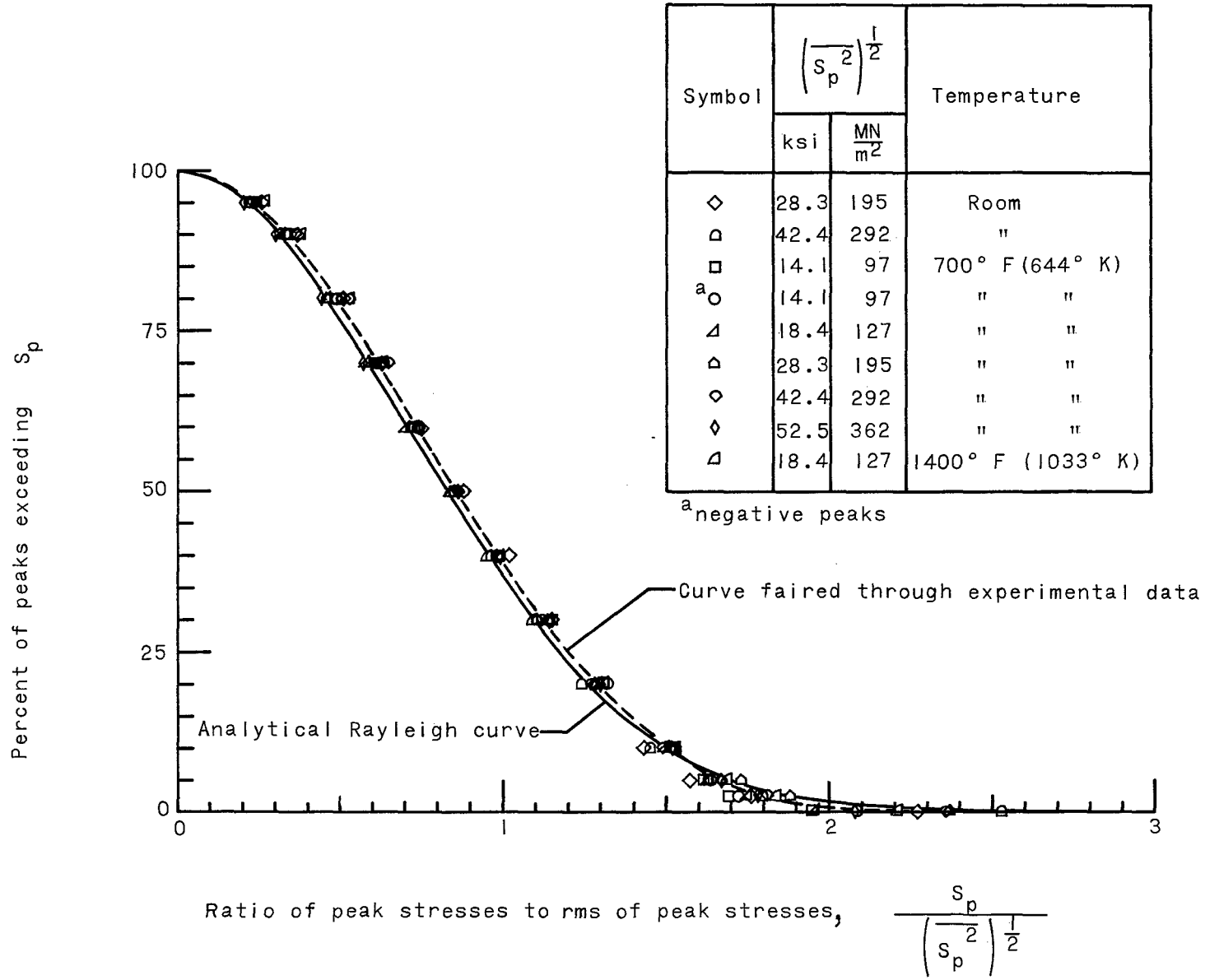

Figure 7.- Results of peak stress measurements for several random-loading tests on René 41 specimens at room and elevated temperatures.

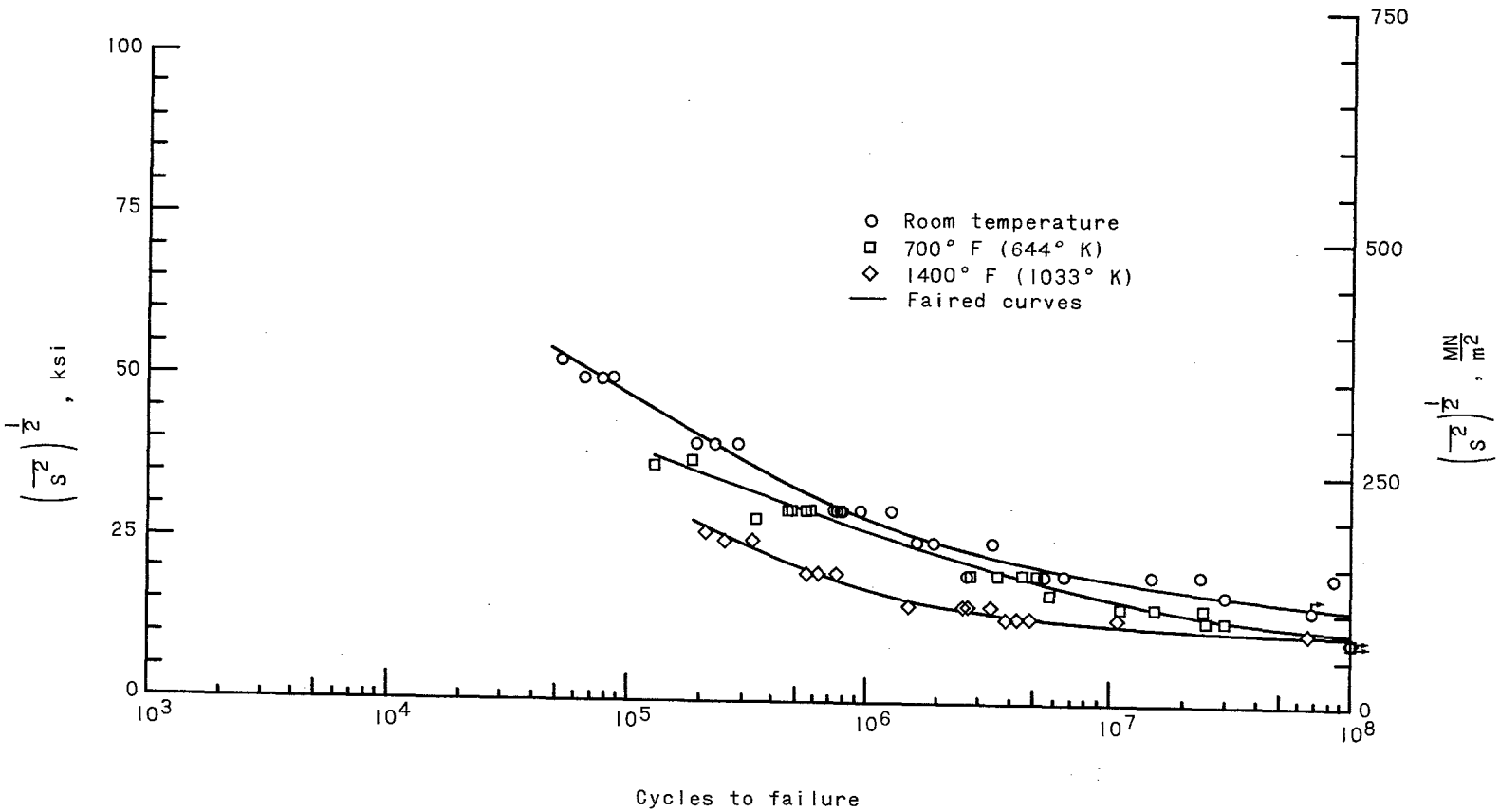

Figure 8.- Results of random-loading fatigue tests on René 41 specimens at room and elevated temperatures.

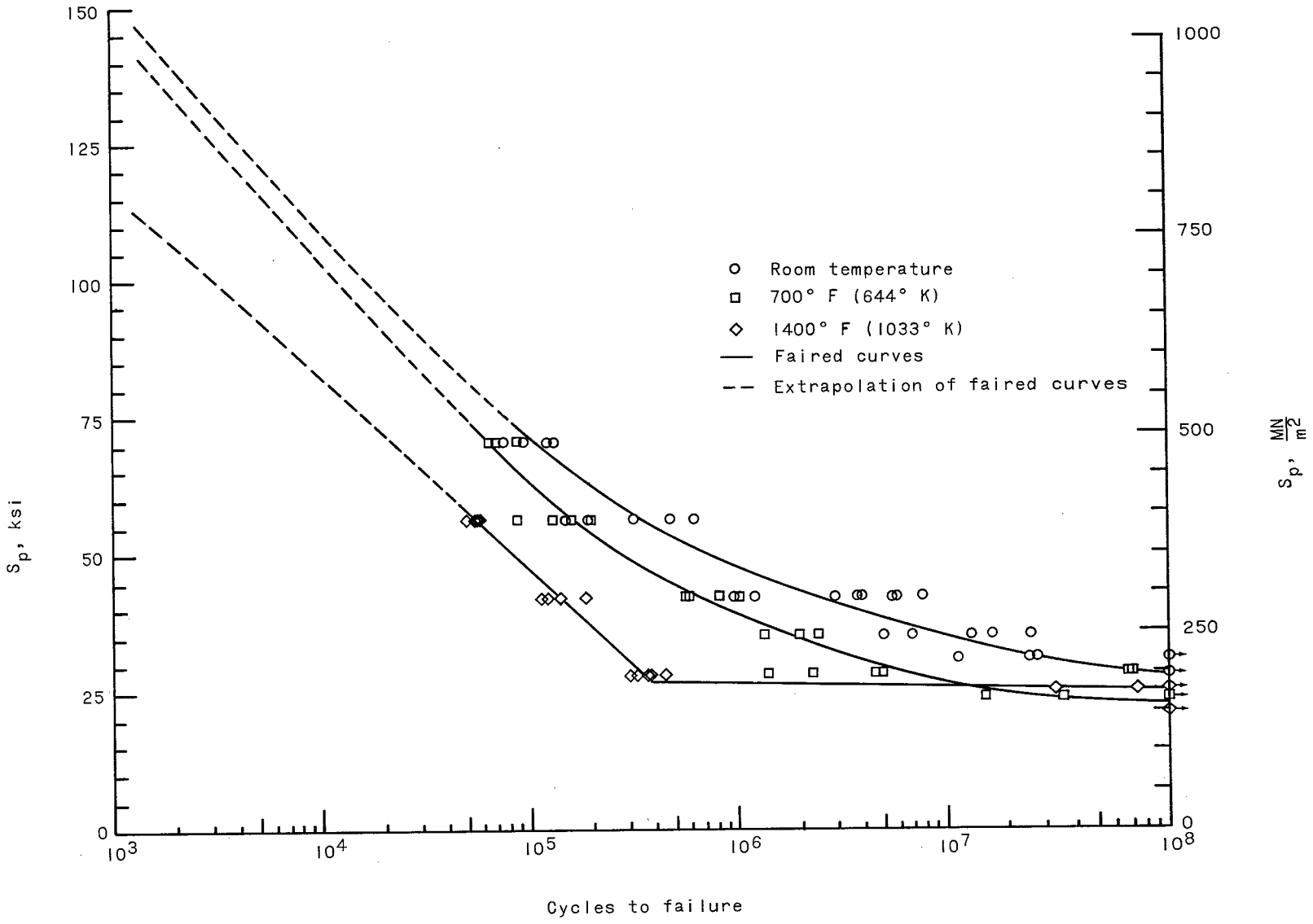

Figure 9.- Results of constant-amplitude fatigue tests on René 41 specimens at room and elevated temperatures.

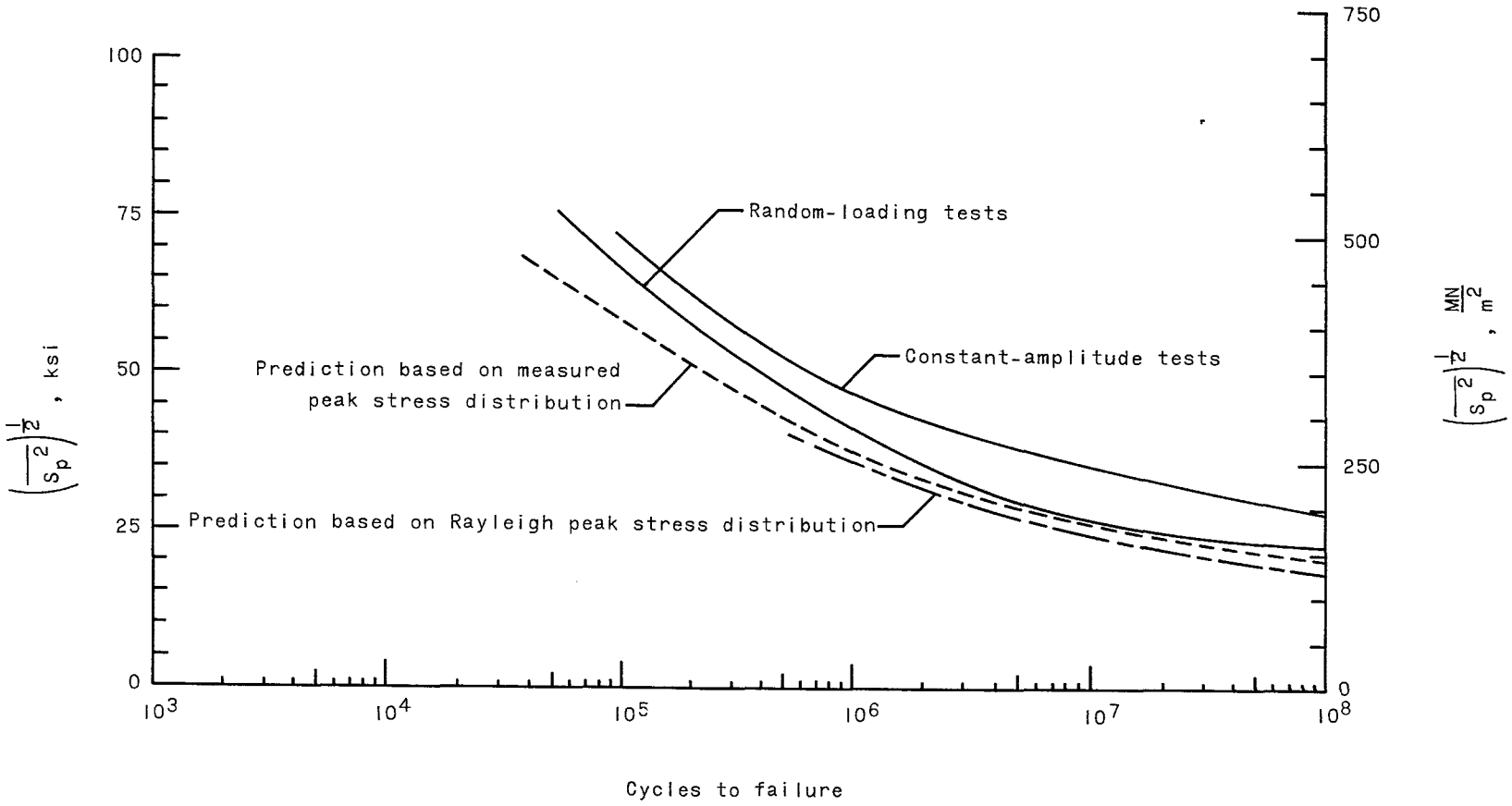

Figure 10.- Comparison of results of room-temperature random-loading tests, constant-amplitude tests, and theoretical predictions of random-loading tests.

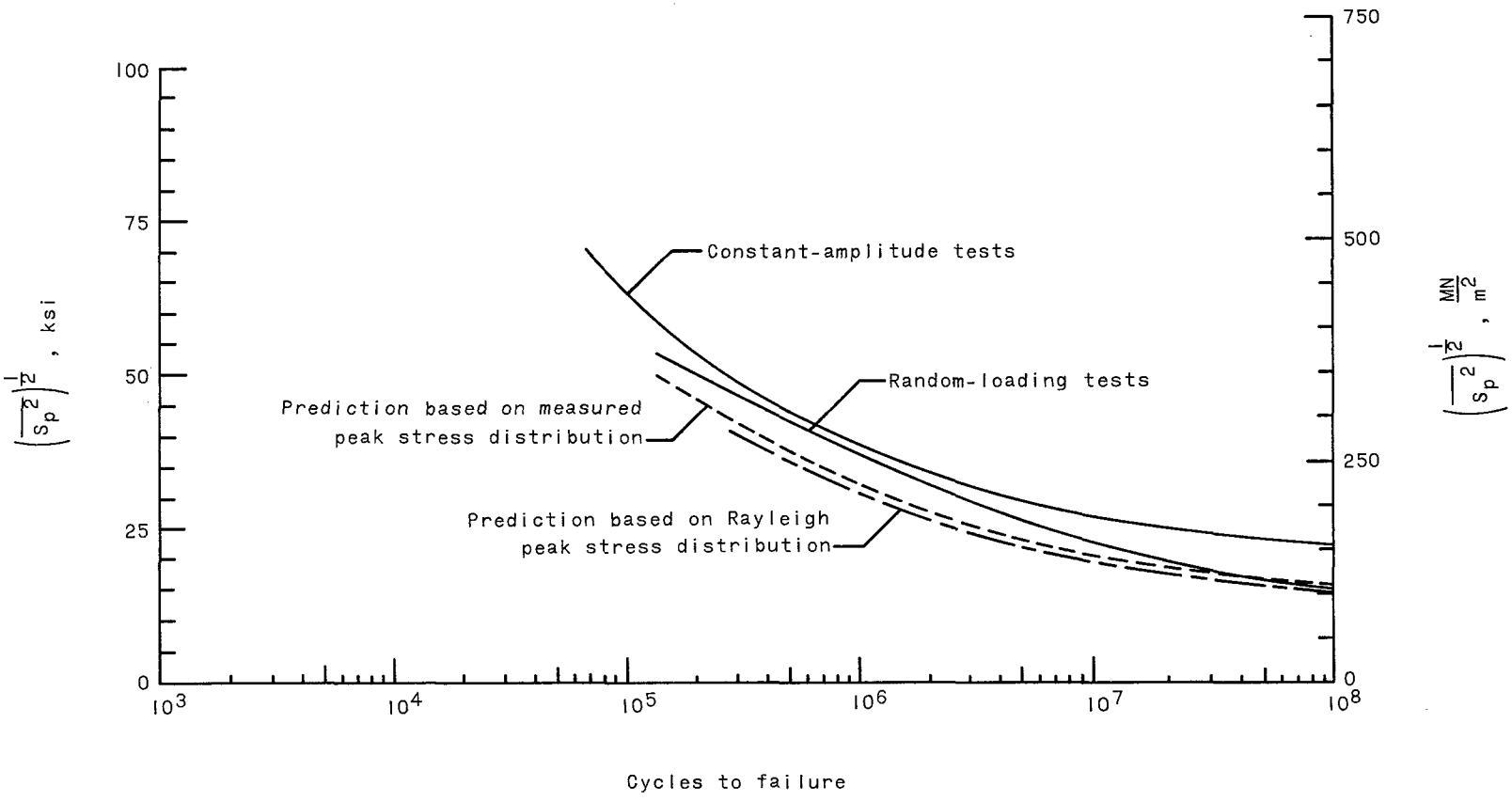

Figure 11.- Comparison of results of 700° F (644° K) random-loading tests, constant-amplitude tests, and theoretical predictions of random-loading tests.

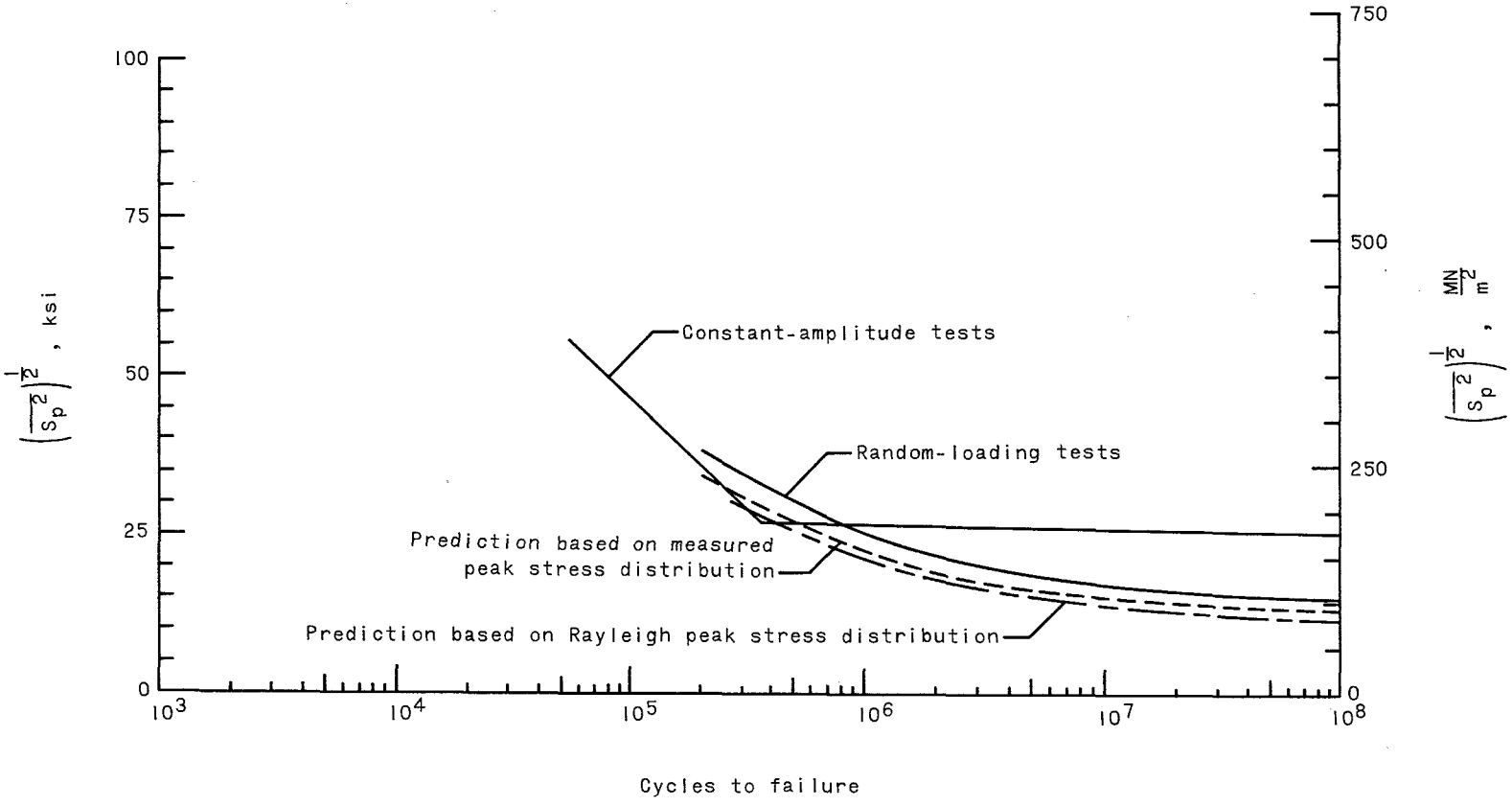

Figure 12.- Comparison of results of 1400° F (1033° K) random-loading tests, constant-amplitude tests, and theoretical predictions of random-loading tests.